

## **UC Irvine**

### **UC Irvine Previously Published Works**

#### **Title**

The shapes and sizes of elliptical galaxy halos from X-ray observations

#### **Permalink**

<https://escholarship.org/uc/item/15s9c7rq>

#### **Journal**

GALACTIC HALOS: A UC SANTA CRUZ WORKSHOP, 136

#### **Authors**

Buote, DA

Canizares, CR

#### **Publication Date**

1998

Peer reviewed

## The Shapes and Sizes of Elliptical Galaxy Halos from X-Ray Observations

David A. Buote

*Institute of Astronomy, Madingley Road, Cambridge CB3 0HA, U.K.*

Claude R. Canizares

*Department of Physics and Center for Space Research 37-241,  
Massachusetts Institute of Technology, 77 Massachusetts Avenue,  
Cambridge, MA 02139*

**Abstract.** We review the theory of how the shapes of the X-ray isophotes probe both the shape and radial distribution of gravitating matter in elliptical galaxies in a way that is more robust than the traditional spherical approach. We summarize and update the previous analyses of X-ray observations of NGC 720 and NGC 1332 and describe preliminary results for NGC 3923.

### 1. Introduction

The soft X-ray band is particularly useful for studying the mass distributions of elliptical galaxies, because the emission over energies  $\sim 0.5 - 2$  keV arises primarily from hot gas with temperature  $T \sim 10^7$  K; i.e. for the more massive ellipticals having ratios of X-ray to blue-band luminosity  $\log_{10} L_x/L_B > \sim -2.7$  (Canizares, Fabbiano, & Trinchieri 1987). The small mean free path ( $\sim \frac{1}{5}$  kpc) indicates that the gas is a collisional fluid with an isotropic pressure tensor. The short sound crossing time ( $< \sim 10^7$  yr) further indicates that, to a good approximation, the gas is in hydrostatic equilibrium. Any streaming motions due to cooling flows or supernova-driven winds should be very subsonic in massive ellipticals; for a recent review see Sarazin (1997).

The traditional method for obtaining the masses of ellipticals from X-rays assumes spherical symmetry and that the X-ray emission arises from a single-phase, non-rotating, ideal gas in hydrostatic equilibrium (Fabricant, Lecar, & Gorenstein 1980),

$$M_{\text{grav}}(< r) \propto rT(r) \left( \frac{d \ln \rho_g}{d \ln r} + \frac{d \ln T}{d \ln r} \right), \quad (1)$$

where  $\rho_g$  is the mass density of the hot gas. The temperature profile,  $T(r)$ , figures prominently in this equation, and has historically hindered reliable mass determinations for most ellipticals. Even at present accurate temperature profiles exist for only a few galaxies and interpretations of these is hampered by the possibilities of cooling flows and multi-temperature gas (Buote & Fabian 1997).

Moreover, if  $\vec{B}$  fields are important then an additional term needs to be added to equation (1). Clearly it is important to find a way to determine  $M_{\text{grav}}$  in a manner that is insensitive to  $T(r)$  and other poorly known properties of the gas.

## 2. A Geometric Test for Dark Matter

The shapes of the X-ray isophotes probe  $M_{\text{grav}}$  without requiring the equation of hydrostatic equilibrium to be solved explicitly. For a galaxy of arbitrary shape the geometric properties of the hydrostatic equation,  $\nabla p_g = -\rho_g \nabla \Phi$ , require that the gas pressure,  $p_g$ , density, and gravitational potential,  $\Phi$ , have the same shapes in three dimensions (3-D) independent of the temperature profile of the gas; this can be shown by taking curls of the hydrostatic equation. (One replaces  $\Phi$  with the appropriate effective potential,  $\Phi_{\text{eff}}$ , if the gas is rotating appreciably.) If the gas is also adequately described by a single-phase,  $p_g = p_g(\rho_g, T)$ , then  $T$  has the same 3-D shapes as  $p_g$ ,  $\rho_g$ , and  $\Phi$ . Since the X-ray emissivity is a function only of these quantities,  $j_x \propto \rho_g^2 \Lambda(T)$  (where  $\Lambda(T)$  is the intrinsic plasma emissivity), we arrive at the key property (Buote & Canizares 1994, §3.1; 1996a, §5.1),

**X-Ray Shape Theorem** *The X-ray emissivity and gravitational potential have the same 3-D shapes independent of the temperature profile of the gas.*

This relation between the shapes of  $j_x$  and  $\Phi$  is more robust to issues like  $\vec{B}$  fields and cooling flows than is equation (1). Although in principle this relation may be affected by arbitrary  $\vec{B}$  fields, it is unaffected if  $p_{\text{mag}} \propto p_g$  as is often assumed (e.g., Loeb & Mao 1994). Similarly, simple models of cooling flows with mass dropout (White & Sarazin 1987) just add another term to  $j_x$  which is only a function of  $\rho_g$  and  $T$ , and thus do not disturb the relation. A possible area of concern for this relation (as well as for equation 1) is if the gas is strongly multi-phase (see §5.).

The X-ray Shape Theorem allows a robust ‘‘Geometric Test’’ for dark matter in ellipticals and galaxy clusters (Buote & Canizares 1994, 1996a). That is, the hypothesis that gravitating mass follows the optical light can be rigorously tested by comparing the shape of the potential,  $\Phi_L$ , constructed from a constant  $M/L$  model with the shape of  $j_x$  obtained from X-ray imaging data. The shape of  $\Phi_L$  depends on both the shape *and* concentration of  $\rho_L$ , the mass density of the constant  $M/L$  model.

This dependence on mass concentration is illustrated in Figure 1 where the potential exterior to a thin ellipsoidal shell with ellipticity,  $\epsilon_\rho = 0.5$ , is shown. The exterior isopotentials are confocal to the shell and thus their ellipticities ( $\epsilon_\Phi$ ) fall to nearly zero at only a few mean radii ( $r$ ) from the shell. (The dotted line is  $\epsilon = 0.5$  at  $5r$  for comparison.) This is an example of the general property that the higher order potential multipoles rapidly decay with increasing distance from a centrally concentrated mass and give way to the spherical monopole. Hence, the ellipticity gradient of the X-ray isophotes, which indicates a related gradient in the potential, probes the radial mass distribution; see Buote & Canizares (1996b) for an application of this idea to clusters.

If the constant  $M/L$  model cannot produce the X-ray isophote shapes for a galaxy, then one can add a dark component until agreement is achieved. Rea-

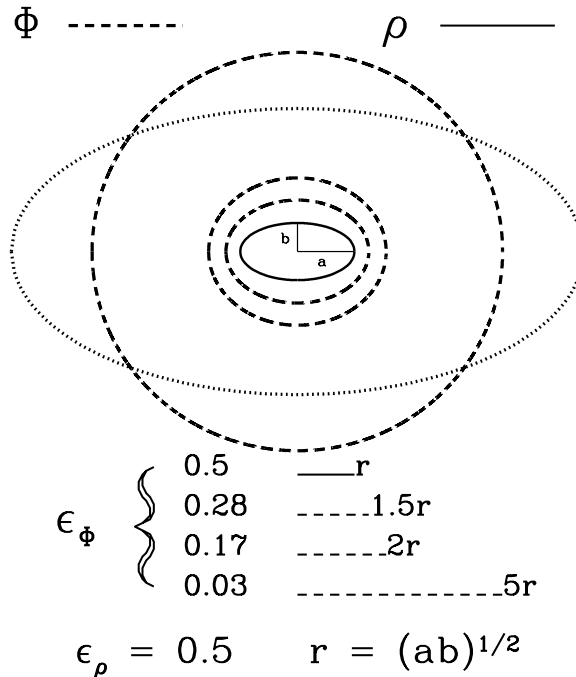


Figure 1. Potential shapes and mass concentration.

reasonable choices for this dark component are a halo having either a NFW density profile (see Navarro, these proceedings) or a Hernquist (1990) profile with the same ellipticity as the light. This approach allows for a lower limit on the ratio of dark to luminous matter,  $M_{DM}/M_L$ , to be determined independent of  $T(r)$ .

Finally, this “Geometric Test” can test the viability of alternative gravity theories like MOND (Milgrom 1983), perhaps the most successful of its kind. Typically these alternative theories are devised to explain radial manifestations of dark matter in galaxies (e.g., spiral galaxy rotation curves). Buote & Canizares (1994) showed that potential shapes in MOND are essentially identical to those in Newtonian theory. Hence, if a constant  $M/L$  model in Newtonian theory is unable to produce the observed X-ray isophote shapes of a galaxy, neither will the corresponding model in MOND.

### 3. Observational Results for the Geometric Test

The isolated E4 galaxy NGC 720 is the prototype for X-ray shape analysis (see Buote & Canizares 1994, 1996c, 1997; Romanowsky & Kochanek 1997). In Figure 2 we show the X-ray contours of the 20ks ROSAT PSPC and 57ks HRI observations of NGC 720 overlaid on the digitized POSS image;  $10'' \sim 1h_{75}^{-1}$  kpc. (The X-ray images have been smoothed for display with Gaussians having half the widths of the respective PSFs; FWHM PSF is  $\sim 30''$  for PSPC and is  $\sim 4''$  for HRI.) The X-ray isophotes are clearly flattened and the orientations appear to be offset from the optical major axis at large radii ( $\sim 100''$ ). Here we

concentrate on the ellipticity of the X-ray surface brightness and defer discussion of the orientations to §6.

Because of the relatively low S/N data of the X-ray images, we use a moment method to compute the ellipticity of the X-ray surface brightness analogous to computing the principal moments of inertia within an elliptical aperture (see Buote & Canizares 1994). The X-ray ellipticity profiles are shown in Figure 2 with  $1\sigma$  error bars from 1000 Monte carlo realizations of the images (see Buote & Canizares 1997); also displayed are the B-band isophotal ellipticities. The ellipticity of the PSPC data is largest and most significant for semi-major axes  $a \sim 90'' - 100''$ , while the HRI measures similar ellipticity down to  $a \sim 40''$ .

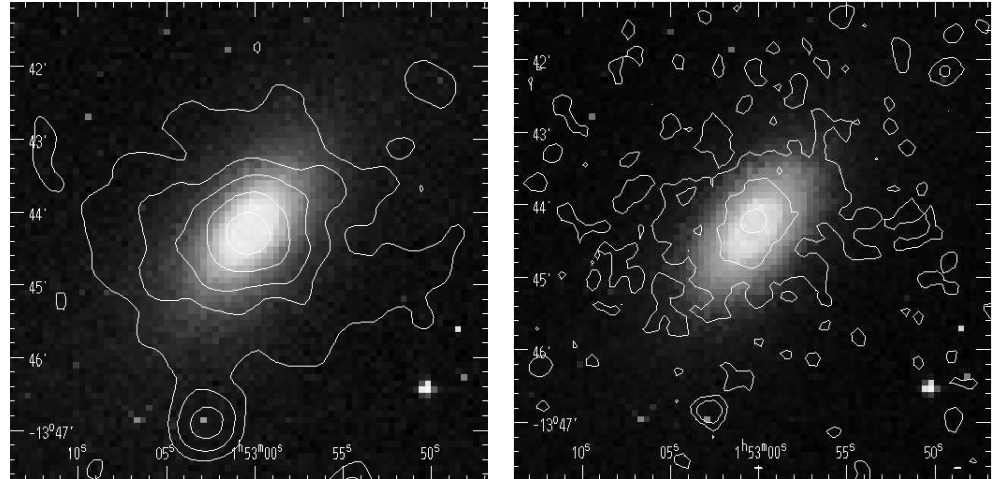
By assuming  $M \propto L_B$  we compute the potential  $\Phi_B$ ; the isopotential ellipticities appear in the figure. The ellipticities of  $\Phi_B$  are considerably smaller than for the B-band light because  $L_B$  is highly centrally concentrated:  $R_e \approx 50''$ , core  $\sim 4''$ . That is, the monopole dominates  $\Phi_B$  for  $r > \sim 10''$ . Since the ellipticities of  $\Phi_B$  fall well below those computed for the X-ray data, the  $M \propto L_B$  model would appear to fail. However, to rigorously implement the Geometric Test we must deproject the X-ray data to compare to the shape of  $\Phi_B$ .

The procedure we adopt, appropriate for the relatively low S/N X-ray data ( $\sim 1500$  counts), is to first jointly fit a simple model to the radial surface brightness of the PSPC and HRI data (e.g., a  $\beta$  model). The best-fit model is deprojected to 3-D and assigned the ellipticities of  $\Phi_B$ . By projecting this ellipsoidal model back onto the sky plane (and adjusting the free parameters to maintain a best fit of the radial surface brightness profile), we obtain a  $M \propto L_B$  model of the X-ray surface brightness. As above, we perform 1000 Monte carlo realizations of this model and compute moment ellipticities,  $\epsilon_x(\Phi_B)$ , analogous to the data to arrive at the  $1\sigma$  error bars in the bottom panels of Figure 2.

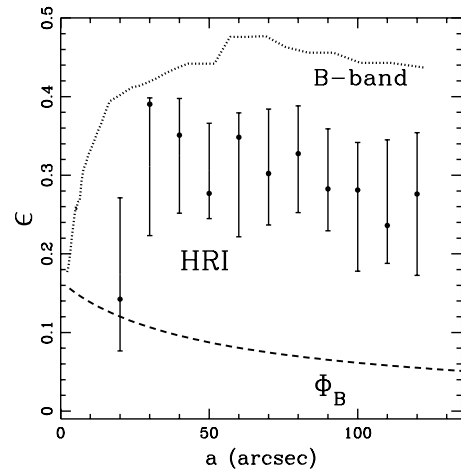
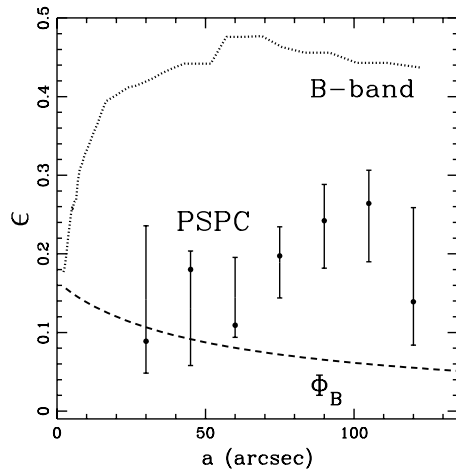
The observed PSPC and HRI ellipticities exceed the  $\epsilon_x(\Phi_B)$  generated by the  $M \propto L_B$  model at greater than the  $3\sigma$  level, thus indicating the need for flattened dark matter. Moreover, even if  $L_B$  is allowed to have ellipticity  $\sim 0.6$ , consistent with the flattest ellipticals observed and expected from stability arguments, this discrepancy cannot be entirely resolved. Hence, in NGC 720 the dark matter must be both flattened and more extended than  $L_B$ , a conclusion independent of the gas temperature profile (Buote & Canizares 1994, 1997).

We have also applied the Geometric Test to PSPC data of the fairly isolated E7/S0 galaxy NGC 1332 (left panels of Figure 3) and to PSPC data of the classic shell galaxy – the isolated E4, NGC 3923 (right panels of Figure 3). Both of these galaxies have lower S/N images than NGC 720 and have smaller measured X-ray ellipticities. Similar to NGC 720, the quite flattened optical light cannot produce flat enough X-ray isophotes. For NGC 1332, the observed PSPC ellipticities exceed the  $\epsilon_x(\Phi_I)$  generated by the  $M \propto L_I$  model at the 90% level and, similar to NGC 720, both flattened and extended dark matter are indicated (Buote & Canizares 1996a). The  $M \propto L_R$  model for NGC 3923 disagrees only at the 80% level. Although this latter case is marginal, the character of the discrepancy is the same (i.e. flattened and extended dark matter needed – Buote & Canizares 1997, to be submitted to ApJ).

Figure 2. NGC 720 PSPC (L) and HRI (R)



X-Ray and Optical Ellipticities



Geometric Test for DM

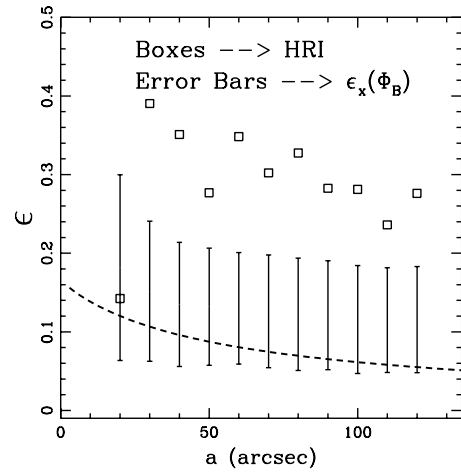
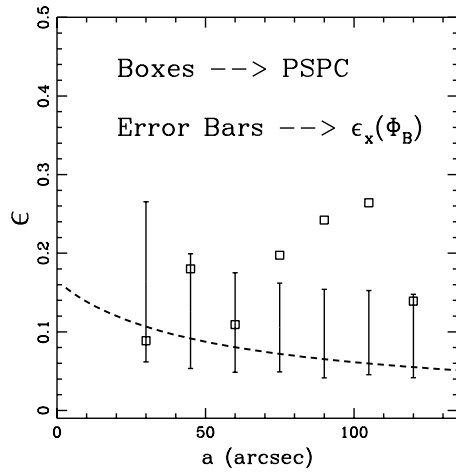
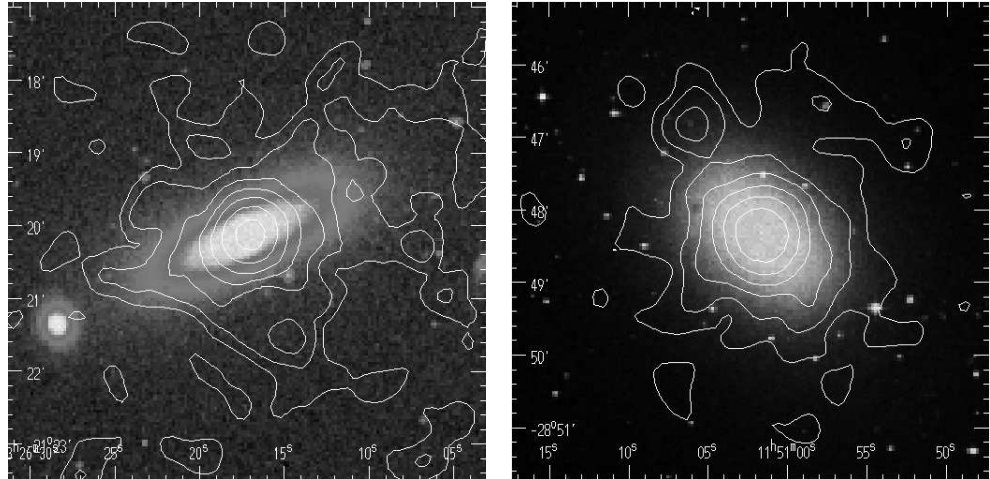
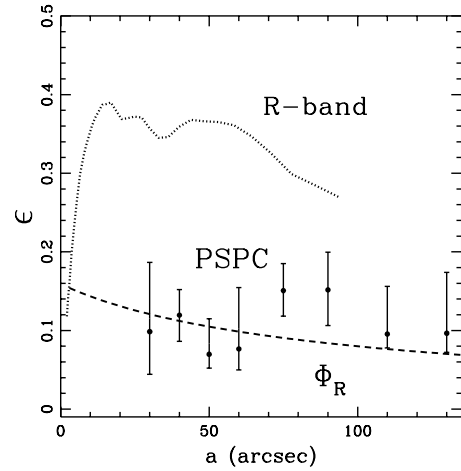
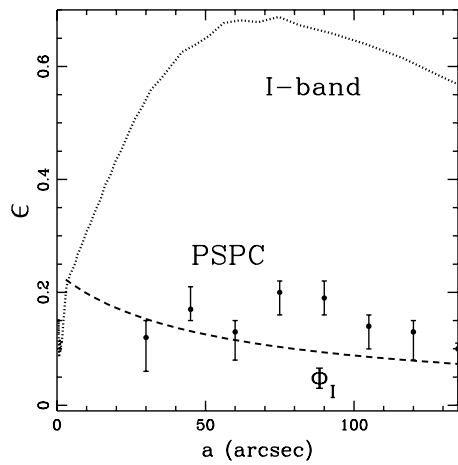


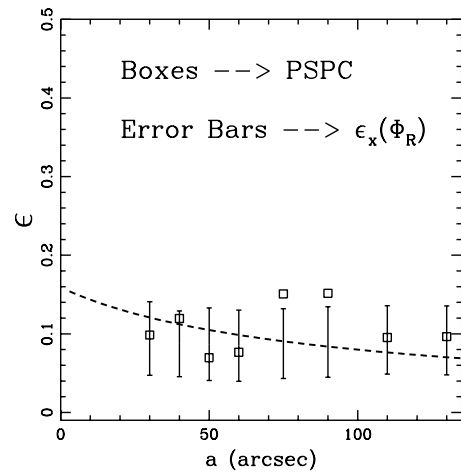
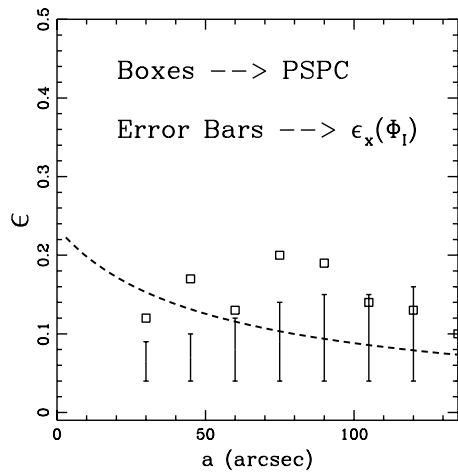
Figure 3. NGC 1332 (L) and NGC 3923 (R)



X-Ray and Optical Ellipticities



Geometric Test for DM



#### 4. Detailed Hydrostatic Models

The Geometric Test robustly examines the need for dark matter and provides some constraints on its shape and extent. To obtain detailed information on the range of allowed shapes and radial profiles for the dark matter the hydrostatic equation must be solved explicitly. Following the pioneering approach of Binney & Strimple (1978), one may solve the hydrostatic equation for the gas density by assuming a single-phase, non-rotating ideal gas,

$$\tilde{\rho}_g = \tilde{T}^{-1} \exp \left( -\Gamma \int_0^{\tilde{x}} \tilde{T}^{-1} \nabla \tilde{\Phi} \cdot d\tilde{x} \right), \quad (2)$$

where  $\Gamma = \mu m_p \Phi(0)/k_B T(0)$  and where, e.g.,  $\tilde{\rho}_g = \rho_g(\tilde{x})/\rho_g(0)$ . Starting with a model for the mass distribution one computes  $\tilde{\Phi}$ , and then, in conjunction with a measurement (or assumption) for the temperature profile, one computes  $\tilde{\rho}_g$ . The model X-ray surface brightness is then obtained by integrating  $\tilde{\rho}_g^2$  along the line-of-sight. This is appropriate since  $\Lambda(T)$  convolved with the ROSAT spectral response is effectively constant for the relevant range of temperatures.

Although not immediately apparent from equation (2), constraints on the *shape* of the mass distribution using this method are quite insensitive to temperature gradients (though not independent of them like the Geometric Test). Strimple & Binney (1979) were the first to show that isothermal and adiabatic ( $p_g \propto \rho_g^{5/3}$ ) temperature profiles lead to approximately similar X-ray isophote shapes. Hence, an isothermal gas may be reasonably assumed if one is only interested in measuring the shape of the gravitating mass.

The results for the ellipticity of the gravitating matter in NGC 720, NGC 1332, and NGC 3923 are shown in Figure 4.. These correspond to oblate spheroidal models with mass density,  $\rho \sim r^{-2}$ , and for an isothermal gas (see Buote & Canizares 1994, 1996a, 1997). (The results do not vary much for other models.) The intensity weighted optical ellipticity (e.g.,  $\langle B \rangle$ ) and the maximum value (e.g.,  $B^{max}$ ) are also shown. One can see that the ellipticity of the gravitating matter is at least as large as that of the light in all three cases, with some indication (especially NGC 720) that the dark matter is more elongated.

Finally, the scale lengths of the gravitating matter are  $\sim 5$  times that of the stellar luminosity for NGC 720, and  $\sim 3$  times for NGC 1332 and  $\sim 2$  times for NGC 3923. These scale length ratios are quoted for Hernquist models to insure a consistent comparison between the light and mass, and the precise values depend on the temperature profile.

#### 5. Caveats

The principal caveats associated with the analysis of X-ray isophote shapes described above are, (1) multi-phase gas, (2) discrete sources, (3) rotation, and (4) environmental effects. There is new evidence from ASCA that the hot gas in the brightest ellipticals consists of at least two temperatures (Buote & Fabian 1997). The single-phase X-ray shape analysis is insensitive to multiple gas phases if either (a) a single phase dominates the emission, (b) (see §2.) the emission is



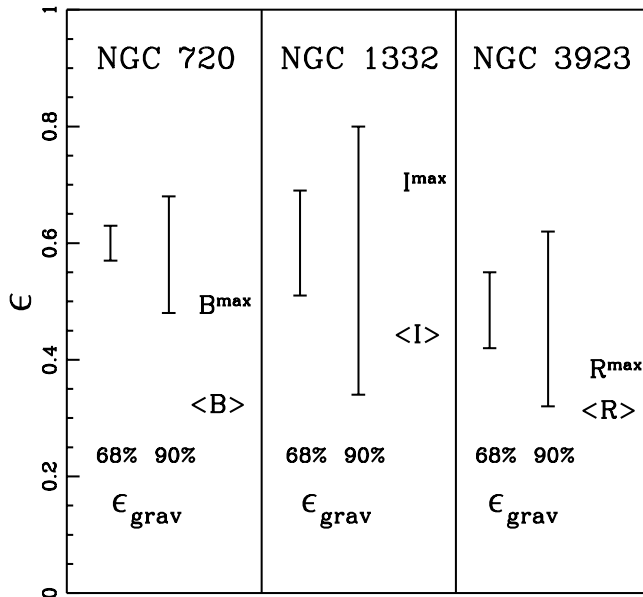


Figure 4. Ellipticity of Gravitating Mass

adequately described as a simple superposition of an ambient phase and a mass dropout term (White & Sarazin 1987), or (c) the phases have similar spatial distributions so that the emission-weighted (or mass-weighted) gas density and temperature are good descriptions of the emissivity; i.e.  $j_x \propto \langle \rho_g \rangle^2 \Lambda(\langle T \rangle)$ . These mean quantities appear to provide a good description of general multi-phase cooling flows in clusters (Thomas, Fabian, & Nulsen 1987).

Discrete sources should contribute to the soft X-ray emission of early-type galaxies. In fact, the ASCA spectra of NGC 720, NGC 1332, and NGC 3923 do require a second thermal component with  $T > \sim 5$  keV suggestive of discrete sources (Buote & Canizares 1997; Buote & Fabian 1997). However, the large inferred temperatures of these hard components in these relatively low S/N galaxies may be a fitting artifact since the highest S/N ellipticals have “hard” components with  $T < \sim 2$  keV which instead indicate another phase of hot gas (Buote & Fabian 1997). Moreover, the spatial distribution of the discrete component has not been accurately measured. However, assuming the discrete sources contribute to 20% of the ROSAT emission of NGC 720 and that they are distributed like the optical light, Buote & Canizares (1997) have shown that the inferred ellipticity of the gravitating mass decreases by only  $\sim 0.05$ .

It is unlikely that rotation plays an important role in the dynamics of NGC 720 and NGC 3923 since the stellar rotation is negligible. Theoretically, even without strong stellar rotation one may (Kley & Mathews 1994) or may not (Nulsen, Stewart, & Fabian 1984) expect a rotating cooling flow to develop depending on whether angular momentum of the gas is conserved. Highly flattened X-ray isophotes indicative of a cooling disk have not been observed. Finally, it

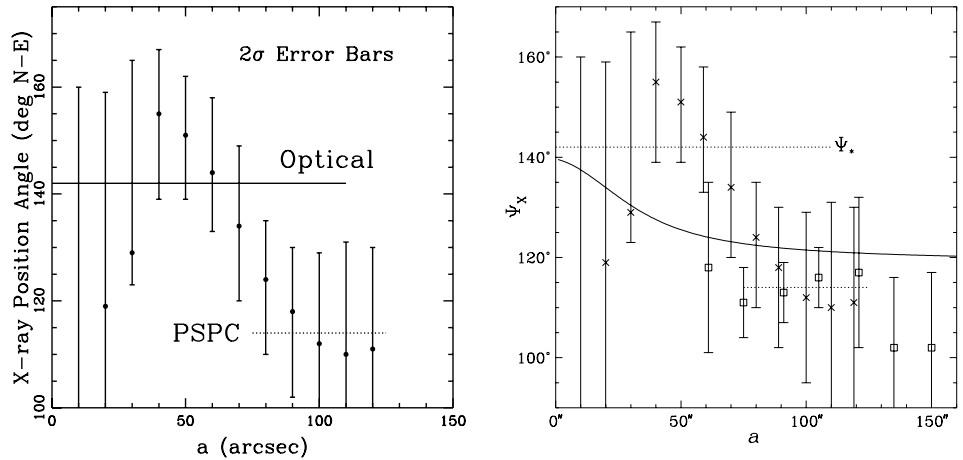


Figure 5. X-Ray Position Angle Twist in NGC 720

is unlikely that environmental effects substantially distort the X-ray isophotes in the isolated ellipticals studied since for  $r < \sim 100''$  no large asymmetries indicative of ram pressure or tidal distortions are observed.

## 6. X-ray position angle twist in NGC 720.

The major axes of the X-ray isophotes of NGC 720 (Figure 2) are offset from the optical major axes. In the left panel of Figure 5 we show the position angle (PA) profile of the HRI data with the PAs of the PSPC and optical data indicated for comparison (Buote & Canizares 1996c). For  $r < \sim 60''$  the X-ray isophotes are aligned with the optical and then twist away to a maximum misalignment of  $\sim 30$  degrees at  $r \sim 100''$ . This misalignment provides further geometric evidence for dark matter. Buote & Canizares (1996c) attempted to explain this PA twist with a simple triaxial halo model where the axial ratio varied as a power law in radius but were unable to simultaneously produce the large twist while maintaining the relatively large X-ray ellipticities.

Romanowsky & Kochanek (1997) have recently examined more detailed physical triaxial models to try to explain the NGC 720 X-ray data. Although the best model of Romanowsky & Kochanek (solid line in right panel of Figure 5) is able to produce a large twist, the twist occurs at very small radii and is thus unable to explain the abrupt twist at  $\sim 60''$  seen in the HRI data. An intrinsic misalignment of the stars and dark matter halo may be implicated.

## 7. Conclusions

X-ray isophote shapes probe both the shape and concentration of gravitating mass essentially independent of the temperature profile of the gas. (The Geometric Test is completely independent of  $T(r)$ .) For the early-type galaxies studied (NGC 720, NGC 1332, NGC 3923), dark matter is required to explain the elongated isophotes. (MOND is unable to escape this manifestation of dark

matter.) The dark matter is at least as flattened as the optical light and is also more extended for each of the galaxies. The X-ray position-angle twist in NGC 720 appears to suggest an intrinsic misalignment of stars and dark matter halo rather than a strongly triaxial system.

This X-ray shape analysis is applicable to isolated early-type galaxies with typical  $\log_{10} L_x/L_B > \sim -2.7$  (i.e. X-rays from hot gas). The next generation X-ray satellites soon to be flown, AXAF and XMM, will have the spatial resolution and effective area to precisely map X-ray isophote shapes for a statistically large sample of galaxies. X-rays are the most promising means on the horizon for obtaining a large sample of gravitating mass shapes and radial mass profiles of early-type galaxies which should significantly enhance our understanding of the structure and formation of these systems (e.g., Sackett 1996; de Zeeuw 1997).

## References

- Binney, J., & Strimple O. 1978, MNRAS, 185, 473  
Buote, D. A., & Canizares, C. R., 1994, ApJ, 427, 86  
Buote, D. A., & Canizares, C. R., 1996a, ApJ, 457, 177  
Buote, D. A., & Canizares, C. R., 1996b, ApJ, 457, 565  
Buote, D. A., & Canizares, C. R., 1996c, ApJ, 468, 184  
Buote, D. A., & Canizares, C. R., 1997, ApJ, 474, 650  
Buote, D. A., & Fabian, A. C., 1997, MNRAS, submitted (astro-ph/9707117)  
Canizares, C. R., Fabbiano, G., Trinchieri, G., 1987, ApJ, 312, 503  
de Zeeuw, P. T., 1997, in Arnaboldi M., Da Costa G. S., and P. Saha, eds.,  
The Nature of Elliptical Galaxies, Proceedings of the Second Stromlo  
Symposium, ASP Conference Series, in press (astro-ph/9704095)  
Fabricant, D., Lecar, M., & Gorenstein, P. 1980, ApJ, 241, 552  
Hernquist, L. 1990, ApJ, 356, 359  
Kley, W., & Mathews, W. G. 1995, ApJ, 438, 100  
Loeb, A., & Mao, S. 1994, ApJ, 435, L109  
Milgrom, M., 1983, ApJ, 270, 365  
Nulsen, P. E. J., Stewart, G. C., Fabian, A. C., 1984, MNRAS, 208, 185  
Romanowsky, A. J., & Kochanek, C. S., 1997, ApJ, in press (astro-ph/9708212)  
Sackett, P. D., 1996, in IAU 173, Gravitational Lensing, ed. C. S. Kochanek, &  
J. N. Hewitt (Dordrecht: Reidel), (astro-ph/9508098)  
Sarazin, C. L., 1997, in Arnaboldi M., Da Costa G. S., and P. Saha, eds.,  
The Nature of Elliptical Galaxies, Proceedings of the Second Stromlo  
Symposium, ASP Conference Series, in press (astro-ph/9612054)  
Strimple, O., & Binney, J. 1979, MNRAS, 188, 883  
Thomas, P., Fabian, A. C., & Nulsen, P. E. J. 1987, MNRAS, 228, 973  
White, R. E. III, & Sarazin, C. L., 1987, ApJ, 318, 621